



TITLE:

# Effects of alloying elements on thermal desorption of helium in Ni alloys

AUTHOR(S):

Xu, Q.; Cao, X.Z.; Sato, K.; Yoshiie, T.

---

CITATION:

Xu, Q. ...[et al]. Effects of alloying elements on thermal desorption of helium in Ni alloys. Journal of Nuclear Materials 2012, 431(1-3): 57-59

ISSUE DATE:

2012-12

URL:

<http://hdl.handle.net/2433/175277>

RIGHT:

© 2011 Elsevier B.V.; この論文は出版社版ではありません。引用の際には出版社版をご確認ご利用ください。; This is not the published version. Please cite only the published version.

# Effects of alloying elements on thermal desorption of helium in Ni alloys

*Q. Xu, X. Z. Cao, K. Sato and T. Yoshiie*

*Research Reactor Institute, Kyoto University, Osaka 590-0494, Japan*

## Abstract

It is well known that the minor elements Si and Sn can suppress the formation of voids in Ni alloys. In the present study, to investigate the effects of Si and Sn on the retention of helium in Ni alloys, Ni, Ni-Si, and Ni-Sn alloys were irradiated by 5 keV He ions at 723 K. Thermal desorption spectroscopy (TDS) was performed at up to 1520 K, and microstructural observations were carried out to identify the helium trapping sites during the TDS analysis. Two peaks, at 1350 and 1457 K, appeared in the TDS spectrum of Ni. On the basis of the microstructural observations, the former peak was attributed to the release of trapped helium from small cavities and the latter to its release from large cavities. Small-cavity helium trapping sites were also found in the Ni-Si and Ni-Sn alloys, but no large cavities were observed in these alloys. In addition, it was found that the oversized element Sn could trap He atoms in the Ni-Sn alloy.

PACS number(s): 61.30.Jf, 61.43.Er, 61.72.jd, 61.72.jj, 61.82.Rx

## 1. Introduction

With the development of spallation target technology, interest in the behavior of helium in solids has increased. Helium is generated in materials by the nuclear reaction of  $(n, \alpha)$ , which increases with increasing neutron energy. Helium, which has a strong interaction with vacancies [1, 2], can form a high density of helium bubbles. Helium, and especially He bubbles, can degrade the ductility and thermal conductivity of a spallation target. Therefore, it is important to find materials with low helium retention and/or better resistance to He bubble formation.

The microstructural evolution in Ni and its binary alloys has been investigated, and it is well known that the minor elements Si and Sn can suppress the formation of voids in Ni alloys [3-8]. The volume size factors, which are the ratio of the difference in volume between the solute and solvent atoms to the volume size of the solvent atom, of Si and Sn in Ni are -5.81% and 74.08% [9], respectively. As Si is an undersized element in Ni, interstitials will be easily trapped by the Si. With increasing dose, a large number of trapped interstitials and their clusters will be formed. These function as effective sites for the annihilation of freely migrating vacancies, and suppress the growth of microvoids [5]. The oversized element Sn, on the other hand, may trap interstitials and vacancies. As a result, the formation of interstitial-type dislocation loops and voids is suppressed due to the recombination of interstitials and vacancies at Sn defect sinks [10].

In the present study, the effects of alloying elements Si and Sn on the accumulation of helium in Ni alloys were investigated.

## 2. Experimental procedure

Pure nickel (99.99%) and its binary alloys containing 2 at% Si and Sn were examined. Well-annealed specimens were irradiated with 5 keV  $\text{He}^+$  ions using an Omegatron gun, in which mono-energetic  $\text{He}^+$  ions were collimated and mass-analyzed [11], at a flux of  $5.0 \times 10^{17} \text{ He}^+/\text{m}^2\text{s}$  to the same nominal dose of  $5.0 \times 10^{19} \text{ He}^+/\text{m}^2$  at 723 K. In addition, to investigate the helium trapping sites in Ni-Sn alloy in detail, He implantation was carried out in both well-annealed samples and samples containing only dislocations. The annealed samples were cold rolled to 10% of their original thickness at room temperature and then annealed at 773 K for 1 h in high vacuum to annihilate vacancies and vacancy clusters. He implantation was then performed at a low energy of 150 eV in order to avoid displacement damage. Afterwards, thermal desorption spectroscopy (TDS) was performed by heating the samples at 1 K/s to 1523 K using infrared irradiation. During heating, the helium release was monitored by a quadrupole mass analyzer. The pressure within the TDS chamber was reduced to below  $1.0 \times 10^{-5} \text{ Pa}$  by vacuum pump before heating the samples. The microstructures of the irradiated samples were investigated using transmission electron microscopy (TEM).

### 3. Results and discussion

No helium desorption peak appeared from un-irradiated Ni, Ni-Si, or Ni-Sn alloys during heating of the samples to 1523 K. Fig. 1 shows helium thermal desorption from Ni (a), Ni-Si (b), and Ni-Sn, (c) after 5 keV  $\text{He}^+$  irradiation to a nominal dose of  $5.0 \times 10^{19} \text{ He}^+/\text{m}^2$  at 723 K. The amount of retained helium in the Ni and binary Ni alloys were calculated based on the TDS data to be  $2.0 \times 10^{19}$  in Ni,  $4.0 \times 10^{19}$  in Ni-Si, and  $3.2 \times 10^{19} \text{ He}/\text{m}^2$  in Ni-Sn, respectively. Two peaks appeared from pure Ni, at about 1350 and 1457 K. Although two peaks also appeared in the Ni-Sn alloy, the first peak shifted to a lower

temperature by 175 K. In the Ni-Si alloy, on the other hand, only one peak appeared. The different helium desorption peaks corresponded to different helium trapping sites. In order to identify these helium trapping sites, TEM observations were carried out. No defects were observed in un-irradiated samples. The microstructures of Ni, Ni-Si, and Ni-Sn after irradiation are shown in Figs. 2, 3, and 4, respectively. In addition, typical microstructures during the annealing of irradiated samples to high temperatures in those alloys are also shown. After irradiation at 723 K, black dots, which are thought to be interstitial-type dislocation loops, were observed in all alloys. Dislocations and cavities with an average diameter of 5 nm and a maximum diameter of 30 nm were observed after annealing irradiated samples at 1223 K, which was just below the temperature of the first peak, as shown in Fig. 1(a), for 5 min in Ni. These cavities grew larger by the Oswald ripening process, to an average diameter of 70 nm after subsequent annealing for 5 min at 1373 K, which was just below the temperature of the second peak, as shown in Fig. 1 (a). According to TEM observations, small and large cavities were formed before 1350 K and 1457 K, respectively, as shown in Fig. 2, and the first and the second peaks of the helium thermal desorption were related to these small and large cavities, respectively. In the Ni-Si alloy, small cavities with an average diameter of 20 nm were observed after annealing an irradiated sample at 1243 K for 5 min, as shown in Fig. 3. This suggests that the helium trapping sites for the peak shown in Fig. 1(b) were small cavities. In the Ni-Sn alloy, dislocations and dislocation loops were observed after annealing an irradiated sample at 1103 K for 5 min, and small cavities with an average diameter of 10 nm were observed after subsequent annealing at 1323 K for 5 min, as shown in Fig. 4. Comparing the microstructural evolution before and after helium thermal desorption, the helium trapping sites for the first and the second peaks of the Ni-Sn alloy appeared to be related to

dislocations and small cavities, respectively. It has been reported that dislocations can also act as helium trapping sites in Ni irradiated by 5 keV  $\text{He}^+$  at room temperature, and helium is released at 940 K during thermal annealing [11]. In order to identify whether the first peak of helium thermal desorption at 1175 K can be attributed to the release of trapped helium from dislocations, TDS measurements were carried out in well-annealed Ni-Sn samples and Ni-Sn samples containing only dislocations. These TDS results each contained a single peak, which was located at 1146 K in He-implanted Ni-Sn alloy and at 1020 K in Ni-Sn alloy containing dislocations, respectively. Therefore, the helium trapping sites for the first peak of Ni-Sn alloy irradiated with 5 keV  $\text{He}^+$  ions were not dislocations, but were the oversized element Sn. Sato et al. reported that Sn atoms act not only as sinks for vacancies, but also as sinks for interstitials [10], and the present results indicate that Sn atoms also act as sinks for interstitial helium.

It is well known that void formation is suppressed in Ni-Si and Ni-Sn alloys, compared with that in Ni [5-8]. In the present study, the nucleation of cavities was delayed in Ni-Si and Ni-Sn alloys relative to that in Ni. In addition, cavities grew during the annealing of irradiated Ni samples at high temperatures; however, the growth of cavities in Ni-Si and Ni-Sn was suppressed. Therefore, helium-vacancy clusters were dispersed in the Ni-Si and Ni-Sn alloys. The migration of helium-vacancy clusters is more difficult than that of free helium or vacancies, so the nucleation of cavities was delayed. Si and Sn alloying elements probably act as trapping sites for helium-vacancy clusters, but it is necessary to investigate the specific interactions of Si and Sn alloying elements with helium and vacancies in more detail.

Although Ni is not a good material for spallation targets, the present results give some information to assist in the selection of a spallation target. For example, the selection of appropriate alloying elements can inhibit the migration of vacancies.

#### 4. Conclusions

In order to investigate the effects of alloying elements on helium retention in Ni and its binary alloys, Ni, Ni-Si, and Ni-Sn were irradiated by 5 keV  $\text{He}^+$  ions at 723 K. The helium trapping sites were cavities in Ni and the Ni-Si alloy, and the oversized element Sn and cavities in the Ni-Sn alloy. Compared with the nucleation and growth of cavities in pure Ni, the addition of an Si or Sn alloying element suppressed the nucleation and growth of cavities.

## References

- [1] M.L. Swanson, J.R. Parsons, C.W. Hoelke, Rad. Eff. 9 (1971) 249.
- [2] N.Q. Lam, P.R. Okamoto, Mater. Res. Soc. Bull. May (1994) 703.
- [3] K. Yamakawa, Y. Shimomura, J. Nucl. Mater. 264 (1999) 319.
- [4] K. Niwase, T. Ezawa, T. Tanabe, J. Nucl. Mater. 212 (1994) 364.
- [5] T. Yoshiie, Q. Xu, Y. Satoh, H. Ohkubo, M. Kiritani, J. Nucl. Mater. 283-287 (2000) 229.
- [6] T. Yoshiie, T. Ishizaki, Q. Xu, Y. Satoh, M. Kiritani, J. Nucl. Mater. 307-311 (2002) 924.
- [7] Q. Xu, T. Yoshiie, J. Nucl. Mater. 307-311 (2002) 380.
- [8] Q. Xu, T. Yoshiie, H. Watanabe, N. Yoshida, J. Nucl. Mater. 367-370 (2007) 361.
- [9] H.W. King, J. Mater. Sci. 1 (1966) 79.
- [10] K. Sato, T. Yoshiie, Q. Xu, J. Japan Inst. Metals 74 (2010) 572.
- [11] X.Z. Cao, Q. Xu, K. Sato, T. Yoshiie, J. Nucl. Mater. 412 (2011) 165.



## Figure Captions

Fig. 1 He thermal desorption in Ni (a), Ni-Si (b), and Ni-Sn (c) irradiated by 5 keV  $\text{He}^+$  ions to  $5.0 \times 10^{19} \text{ He}^+/\text{m}^2$  at 723 K.

Fig. 2 Microstructures in Ni after irradiation and annealing. (a) after irradiation by 5 keV  $\text{He}^+$  ions to  $5.0 \times 10^{19} \text{ He}^+/\text{m}^2$  at 723 K; (b) irradiated sample annealed at 1223 K for 5 min; (c) irradiated sample after subsequent annealing at 1373 K for 5 min.

Fig. 3 Microstructures in Ni-Si after irradiation and annealing. (a) after irradiation by 5 keV  $\text{He}^+$  ions to  $5.0 \times 10^{19} \text{ He}^+/\text{m}^2$  at 723 K; (b) irradiated sample annealed at 1243 K for 5 min.

Fig. 4 Microstructures in Ni-Sn after irradiation and annealing. (a) after irradiation by 5 keV  $\text{He}^+$  ions to  $5.0 \times 10^{19} \text{ He}^+/\text{m}^2$  at 723 K; (b) irradiated sample annealed at 1103 K for 5 min; (c) irradiated sample after subsequent annealing at 1323 K for 5 min.

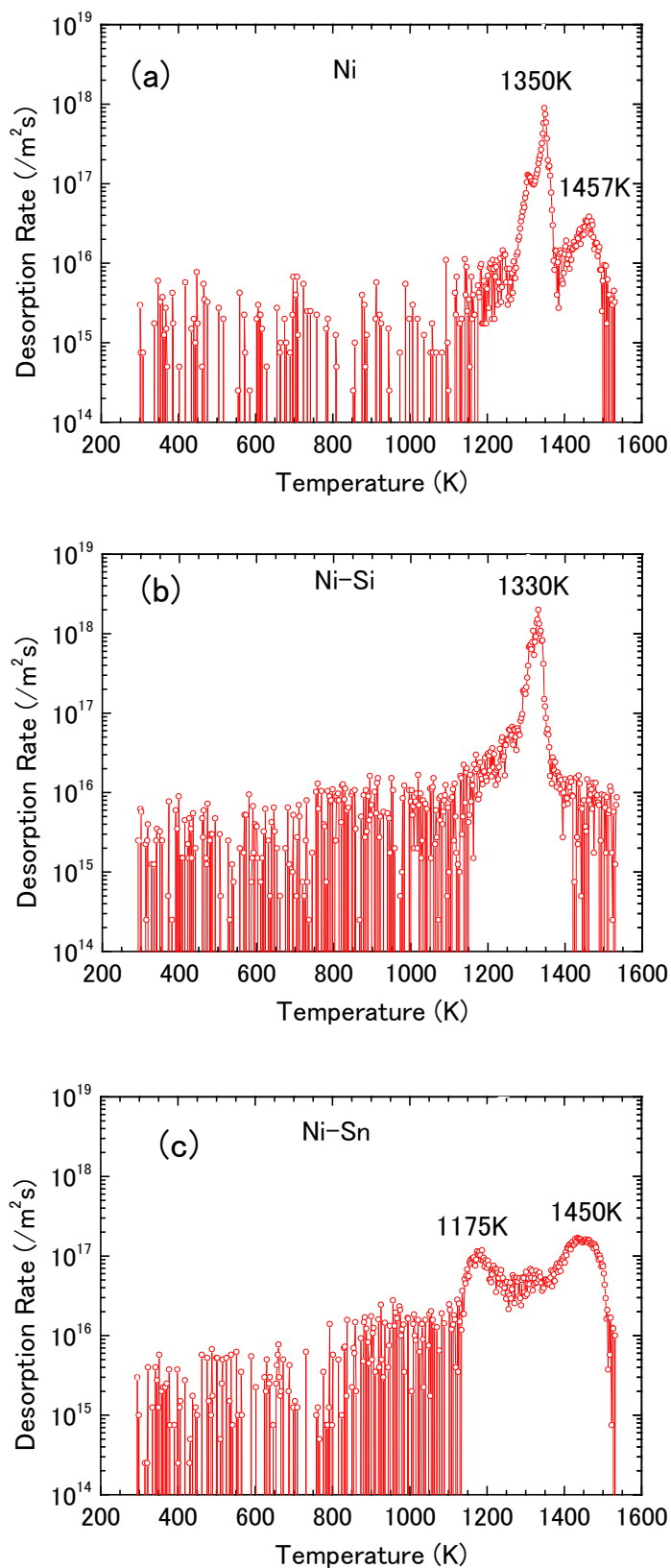


Fig. 1 He thermal desorption in Ni (a), Ni-Si (b) and Ni-Sn (c) irradiated by 5 keV He<sup>+</sup> ions to  $5.0 \times 10^{19}$  He<sup>+</sup>/m<sup>2</sup> at 723 K.

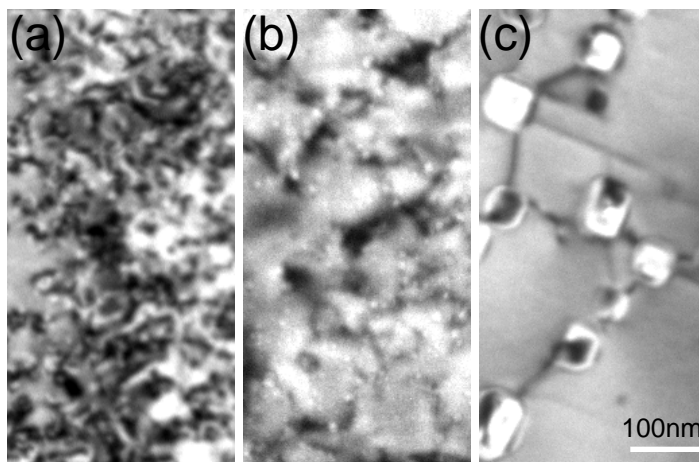


Fig. 2 Microstructures in Ni after irradiation and anneal.  
(a) after irradiated by 5 keV He<sup>+</sup> ions to  $5.0 \times 10^{19}$  He<sup>+</sup>/m<sup>2</sup> at 723 K;  
(b) irradiated sample annealed at 1223 K for 5 min;  
(c) irradiated sample after subsequent annealing at 1373 K for 5 min.

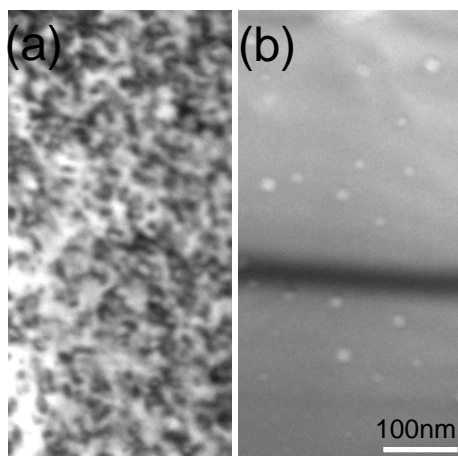


Fig. 3 Microstructures in Ni-Si after irradiation and anneal.  
(a) after irradiated by 5 keV He<sup>+</sup> ions to  $5.0 \times 10^{19}$  He<sup>+</sup>/m<sup>2</sup> at 723 K;  
(b) irradiated sample annealed at 1243 K for 5 min.

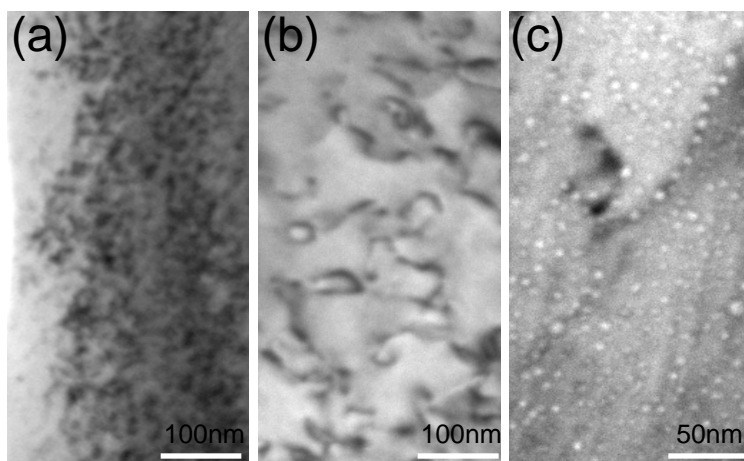


Fig. 4 Microstructures in Ni-Sn after irradiation and anneal.  
(a) after irradiated by 5 keV He<sup>+</sup> ions to  $5.0 \times 10^{19}$  He<sup>+</sup>/m<sup>2</sup> at 723 K;  
(b) irradiated sample annealed at 1103 K for 5 min;  
(c) irradiated sample after subsequent annealing at 1323 K for 5 min.